Biomaterials and Biomechanics in Bioengineering, *Vol. 2, No. 2 (2015) 111-125*
(Formerly, Biomaterials and Biomedical Engineering)
DOI: http://dx.doi.org/10.12989/bme.2015.2.2.111

Parametric study of porous media as substitutes for flow-diverter stent

Makoto Ohta[*1], Hitomi Anzai[1,2a], Yukihisa Miura[3b] and Toshio Nakayama[4,5c]

[1]*Institute of Fluid Science, Tohoku University, 2-1-1 Katahira, Aoba-ku Sendai, Miyagi, 980-8577, Japan*
[2]*Frontier Research Institute for Interdisciplinary Sciences, Tohoku University, 6-3 Aramaki Aza Aoba, Aoba-ku, Sendai, Miyagi 980-8578, Japan*
[3]*Graduate School of Engineering, Tohoku University, 6-6, Aramaki Aza Aoba, Aoba-ku, Sendai, Miyagi 980-8579, Japan*
[4]*Graduate School of Biomedical Engineering, Tohoku University, 6-6, Aramaki Aza Aoba, Aoba-ku, Sendai, Miyagi 980-8579, Japan*
[5]*National Institute of Technology, Tsuruoka College, 104 Sawada, Inooka, Tsuruoka, Yamagata 997-8511, Japan*

(Received April 4, 2015, Revised June 12, 2015, Accepted June 13, 2015)

Abstract. For engineers, generating a mesh in porous media (PMs) sometimes represents a smaller computational load than generating realistic stent geometries with computer fluid dynamics (CFD). For this reason, PMs have recently become attractive to mimic flow-diverter stents (FDs), which are used to treat intracranial aneurysms. PMs function by introducing a hydraulic resistance using Darcy's law; therefore, the pressure drop may be computed by test sections parallel and perpendicular to the main flow direction. However, in previous studies, the pressure drop parallel to the flow may have depended on the width of the gap between the stent and the wall of the test section. Furthermore, the influence of parameters such as the test section geometry and the distance over which the pressure drops was not clear. Given these problems, computing the pressure drop parallel to the flow becomes extremely difficult. The aim of the present study is to resolve this lack of information for stent modeling using PM and to compute the pressure drop using several methods to estimate the influence of the relevant parameters.

To determine the pressure drop as a function of distance, an FD was placed parallel and perpendicular to the flow in test sections with rectangular geometries. The inclined angle method was employed to extrapolate the flow patterns in the parallel direction. A similar approach was applied with a cylindrical geometry to estimate loss due to pipe friction. Additionally, the pressure drops were computed by using CFD. To determine if the balance of pressure drops (parallel vs perpendicular) affects flow patterns, we calculated the flow patterns for an ideal aneurysm using PMs with various ratios of parallel pressure drop to perpendicular pressure drop. The results show that pressure drop in the parallel direction depends on test section. The PM thickness and the ratio of parallel permeability to perpendicular permeability affect the flow pattern in an ideal aneurysm. Based on the permeability ratio and the flow patterns, the pressure drop in the parallel direction can be determined.

*Corresponding author, Associate Professor, E-mail: ohta@biofluid.ifs.tohoku.ac.jp
[a]Assistant Professor, E-mail:anzai@biofluid.ifs.tohoku.ac.jp
[b]MSc. Student, E-mail:miura@biofluid.ifs.tohoku.ac.jp
[c]Assistant Professor, E-mail: nakayama@tsuruoka-nct.ac.jp

http://www.techno-press.org/journals/bme&subpage=7 ISSN: 2288-3738 (Print), 2288-3746 (Online)

Keywords: intracranial stent; porous media; flow diverter; cerebral aneurysm; Darcy's law

1. Introduction

A flow-diverter stent (FD) is an intracranial stent used to treat cerebral aneurysm. Recently, FDs have become attractive because they apparently reduce the flow into an aneurysm (Sadasivan *et al*. 2009). To improve this treatment, researchers would like to use computational fluid dynamics (CFD) to calculate any changes in flow patterns after FD placement (Karmonik *et al*. 2013, Kulcsar *et al*. 2012, Ma *et al*. 2012, Xu *et al*. 2013, Zhang *et al*. 2013). The use of FDs also poses several problems such as occlusion of the parent artery or rupture of the aneurysm just after FD placement (Cebral *et al*. 2011). Because these difficulties are strongly related to blood flow, flow simulation by CFD is an attractive method to study FDs. Such flow simulations generally define geometries of aneurysms and stents in the computation by creating calculation meshes in the fluid space (Hassan *et al*. 2004). However, the meshing process is lengthy and generates a heavy computational load, particularly for the small gaps between stent struts.

Augsburger *et al*. (2011) introduced the concept of employing porous media (PMs) to mimic a stent (Augsburger *et al*. 2011). If a PM is placed in the neck instead of a stent, a unified mesh instead of a boundary-fitted mesh can be generated, which reduces the associated computational load. Furthermore, Augsburger et al. report that the flow pattern generated by PMs in aneurysms is similar to that generated by stents.

In the same study, Augsburger et al. computed the pressure drop associated with stents by applying Darcy's law to test sections to calculate the hydraulic resistance of the PM. Fig. 1 shows the test section employed in their study to compute the pressure drop (Augsburger *et al*. 2011). To use Darcy's law, the pressure drop must be known in the direction parallel and perpendicular to the flow. The pressure drop in the perpendicular direction due to a stent (hereafter called the perpendicular pressure drop) is simple to compute: a stent mesh is placed in the cylindrical test section and the pressure drop is the difference between upstream and downstream hydrodynamic pressure. Augsburger *et al*. (2011) describe a few methods to compute the pressure drop based on the simulation results. Furthermore, to compute the pressure drop in the parallel direction due to a stent (hereafter called the parallel pressure drop), a stent was placed parallel to the test section, as shown in Fig. 1(b). In this case, the parallel pressure drop is affected by many parameters such as the distance between upstream and downstream of the stent and the size of gaps between the stent

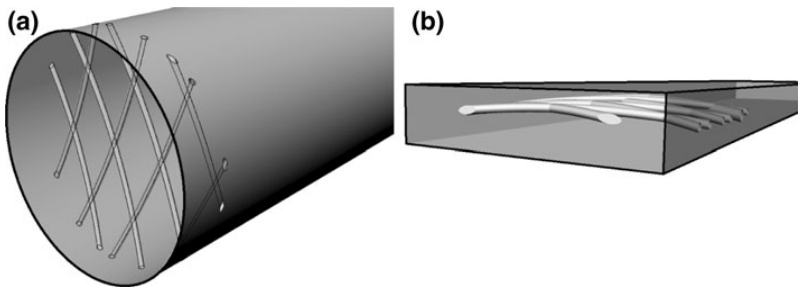

Fig. 1 Test sections for computing pressure drop due to stent. (a) and (b) show the sections in the perpendicular and parallel direction, respectively (Augsburger *et al*. 2011)

and the wall of the test section. Furthermore, the flow patterns in an aneurysm under the various conditions remain unclear. Therefore, parametric studies can yield useful information for developing a method for replacing stents with PMs.

The goal of the present study is thus to substitute this lack of information for modeling stents with PMs. To this end, we calculate the flow resistance of stents using test sections described by various parameters such as test-section geometry and length. To understand how the various parameters influence the results, the flow patterns in an ideal aneurysm model are compared using PMs and conventional CFD with stents.

2. Methods

2.1 Conventional CFD as benchmark

To establish a benchmark against which we can compare our results, we employed a conventional CFD approach with Fluent 6.3 (Ansys Inc., US). The stent in this case comprised a flat screen as defined by the 3D CAD software Pro/ENGINIER Wildfire 4.0 (PTC, Needham, US). A silk stent (Balt International, Montmorency, France) was used as a reference. The geometry of this stent is shown in Fig. 2. The strut width was 25 μm and struts were spaced 250 μm apart.

2.2 Geometry of aneurysm and parent artery

An ideal aneurysm model was used. The parent artery is 4 mm in diameter and 100 mm from inlet to outlet. The radius of the aneurysm sack, the neck diameter, and the height of the aneurysm sac are 5, 5, and 10 mm, respectively (Fig. 3). Models such as this with a straight tube as a parent artery and a sphere as an aneurysm sac have already been used by several groups (Anzai *et al*. 2014, Lee *et al*. 2014).

2.3 Mesh generation

The stent model and PM domain were positioned at the neck plane to cover the aneurysmal orifice. The surface mesh of the stent was generated by Tgrid (5.0 Ansys Inc., US), and the volume

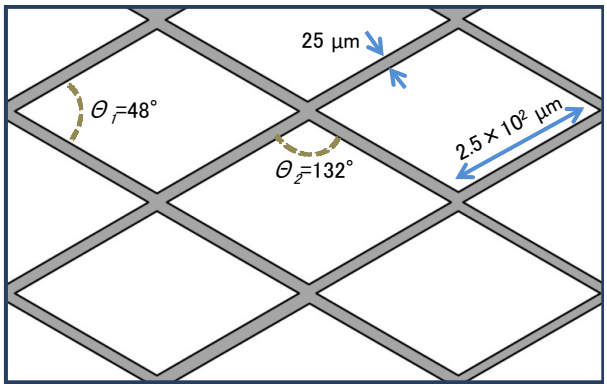

Fig. 2 Configuration of stent struts

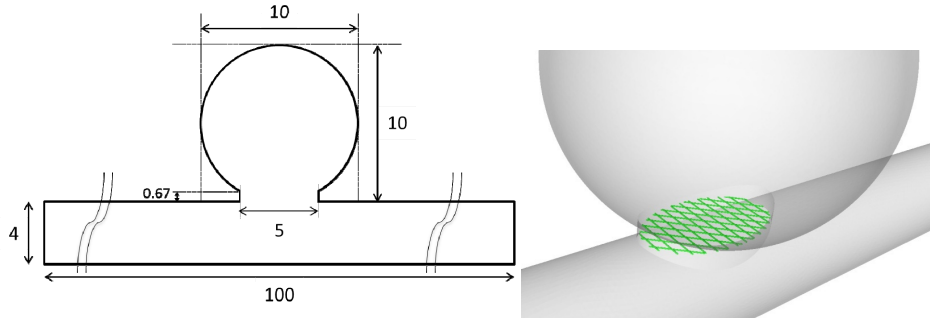

Fig. 3 Configuration of cerebral artery with aneurysm and stent (a unit is mm). The left image shows the model geometry for parent artery and an aneurysm. The right image shows the aneurysm neck with stent

meshes in the ideal aneurysm and parent artery with stent and PM were generated by Gambit (2.4, Ansys Inc., US). The volume meshes contained fine structure around the stent. Table 1 shows the number of mesh.

2.4 Porous medium and Darcy's law

The flow in the PM domain was modeled by adding a momentum source term to the standard fluid flow Navier-Stokes equations. This term contains a viscous resistance term and an inertial resistance term, as follows

$$\Delta p = \left(\frac{\mu}{\alpha} v_i + C_2 \frac{1}{2} \rho v_i^2 \right) \Delta e \tag{1}$$

where i is the ith (x, y, or z) coordinate, v is the velocity, α is the permeability, C_2 is the inertial resistance factor, μ is the viscosity, ρ is the fluid density, and Δe is the thickness of the PM domain. If the pressure drop is approximated as

$$\Delta p = a v^2 + b v \tag{2}$$

we can obtain the two pressure coefficients $1/\alpha$ and C_2.

2.5 Parallel and perpendicular pressure drops vs distance

To compute the pressure drop due to the stent, two surfaces were defined in the test section: one in front of the stent and one in the back of the stent. The distance ΔL between the two surfaces was varied to examine the relationship between pressure drop and ΔL.

2.6 Computing parallel pressure drop by inclined angle method

The parallel direction may be estimated as the extrapolated angle (0°) with respect to the perpendicular direction (90°), as shown in Fig. 4. The parallel pressure drop was measured using the inclined angle method.

Table 1 The number of mesh of each sample

	Mesh numbers
Stent	7.6×10^6
PM: Δe=25 μm	9.8×10^6
PM: Δe=50 μm	3.7×10^6
PM: Δe=100 μm	3.2×10^6
PM: Δe=200 μm	2.6×10^6

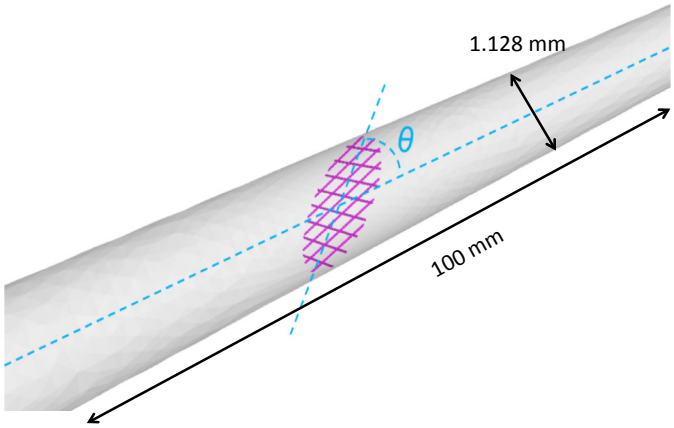

Fig. 4 Schematic diagram for inclined angle method

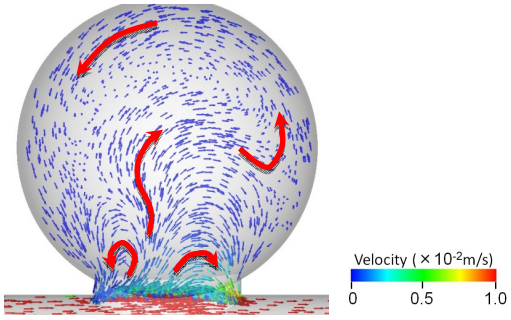

Fig. 5 Flow patterns with stent model. The flow is from left to right in the parent artery

2.7 Parallel pressure drop vs diameter of test section

The diameter of the test section may influence the results for the pressure drop, particularly for the parallel direction because of pipe-friction loss. To evaluate this effect, a stent was placed in test sections of various diameters and the pressure drop was calculated for each.

2.8 Ratio of parallel pressure drop to perpendicular pressure drop

In the study by Augsburger *et al*. (2011), the PM domain seems to be thicker than a real stent,

yet the resulting flow pattern is fit to that of a real stent. This finding suggests that the thickness of the PM affects the flow pattern and the pressure drop ratio for PMs. To determine how the ratio of parallel to perpendicular pressure drop coefficients affects the flow patterns, the latter are calculated for various pressure drop ratios. First, the ratios are set between 1 and 5 using

$$Ratio = \frac{1/\alpha_{perpendicular}}{1/\alpha_{parallel}} = \frac{\alpha_{parallel}}{\alpha_{perpendicular}} \tag{3}$$

Next, the parallel pressure drop and the parameters $1/\alpha$ and C_2 are calculated using the results for perpendicular pressure drop. If the ratio increases, the permeability in the parallel direction increases.

2.9 CFD conditions

The blood flow of all calculations were simplified as isothermal, incompressible and laminar Newtonian flow with a density of 1050 kg/m^3 and a viscosity of 3.5×10^{-3} Pa·s. The inlet boundary was constant with velocity of 0.25 m/s and flow conditions were uniform with a Reynolds number of 300. Pressure condition of 0 Pa was set at the model outlet which is the condition of traction free. Stationary and no-slip condition was set on the model wall. These conditions were similar to previous papers (Anzai *et al*. 2010, Augsburger *et al*. 2011, Yujie *et al*. 2014).

3. Results

3.1 Control flow pattern (flow with stent)

Fig. 5 shows flow patterns obtained by the stent model. The flow enters from the distal neck and two vortices appear in the aneurysm. The bigger vortex is rotated anticlockwise and the smaller vortex is rotated clockwise. Fig. 6 shows a 0.1 m/s velocity isosurface. A bigger bump in the isosurface appears in the distal neck and a smaller bump appears in the proximal neck. These results are consistent with previous studies (Anzai *et al*. 2014, Augsburger *et al*. 2011, Yujie *et al*. 2014).

3.2 Perpendicular direction

Fig. 7 shows the pressure drop as a function of distance between calculation surfaces. Calculation surfaces spaced by less than 400 μm result in a larger pressure drop, whereas the pressure drop is relatively stable for calculation surfaces spaced more than 400 μm apart. This finding indicates that the effect of the stent becomes negligible for separations greater than 400 μm.

Fig. 8 shows contour maps of the velocity and pressure distributions in a perpendicular test section for an inlet velocity of 0.5 m/s. The black line shows the calculation surfaces at 400 μm. The struts form narrow channels, which lead to jet flow between the struts. However, the flow speed returns to normal after approximately 400 μm. Lower pressure is also observed between the struts.

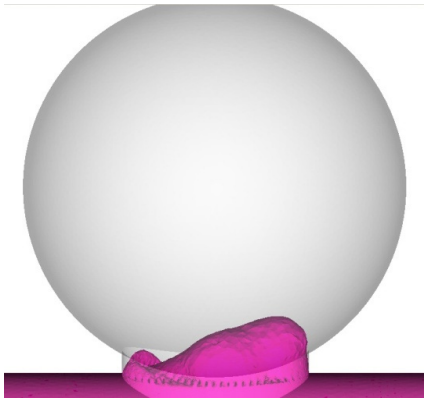

Fig. 6 Velocity isosurface (0.1 m/s). The flow is from left to right in the parent artery

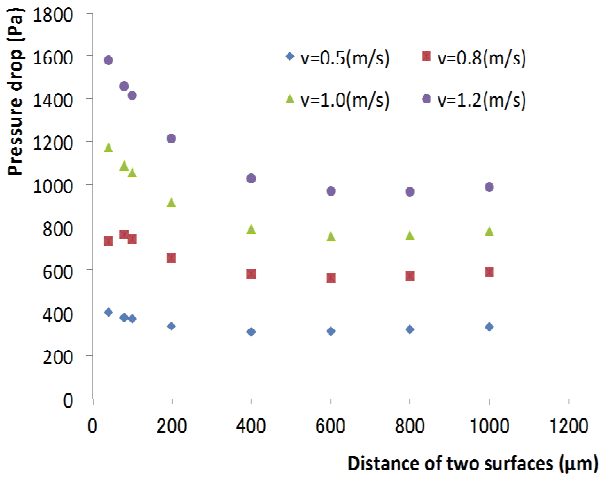

Fig. 7 Pressure drop as a function of distance between calculation surfaces

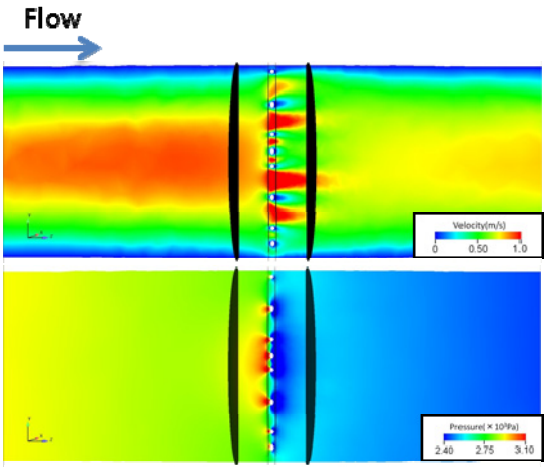

Fig. 8 Contour map of velocity (upper) and pressure (lower) distributions for perpendicular test section in the center plane with inlet velocity of 0.5 m/s

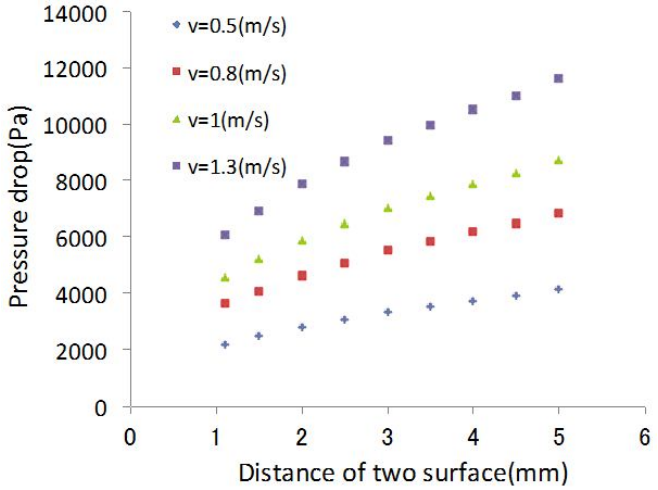

Fig. 9 Pressure drop as a function of distance between calculation surfaces

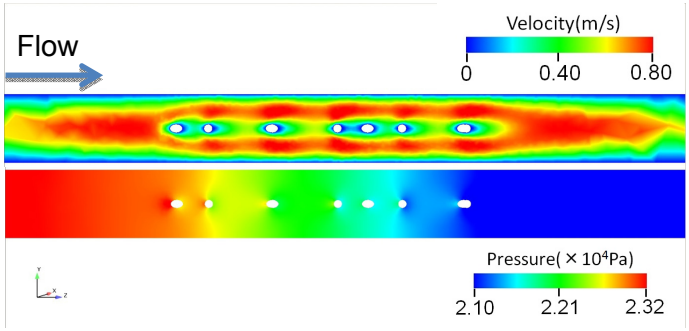

Fig. 10 Contour maps of velocity distribution (upper) and pressure distribution (below) of parallel test section in the center plane at inlet velocity of 0.5 m/s

3.3 Parallel direction

Fig. 9 shows the parallel pressure drop. The pressure drop increases almost linearly with distance between calculation surfaces, which differs from the results for the perpendicular section. This increase may depend on the thickness of the test section because the gap between the stent and the wall of the test section is too thin.

Fig. 10 shows contour maps of velocity and pressure for a parallel test section with an inlet velocity of 0.5 m/s. Higher speed flow is observed between the wall of the test section and the struts but not between the struts. This result indicates that the flow entering the test section is separated into top and bottom flow by the strut line, and the fluid passes mainly through the gaps between the line of struts and the walls of the test section. As shown in Fig. 9, the pressure drop gradually increases along the length of the test section because of wall friction, and the pressure distribution across the cross section of the test section is relatively constant. The parallel pressure drop depends on not only the stent length, but also the separation of the calculation surfaces, and the size of the gap between the wall of the test section and the stent. Thus, calculating the pressure drop based on stent thickness in this test section is difficult.

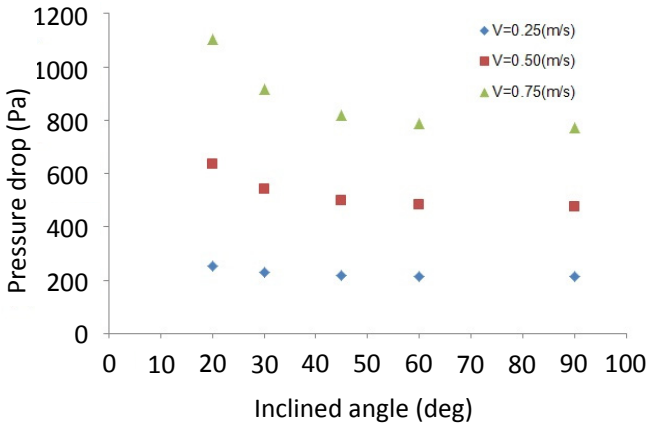

Fig. 11 Pressure drop as a function of inclined angle

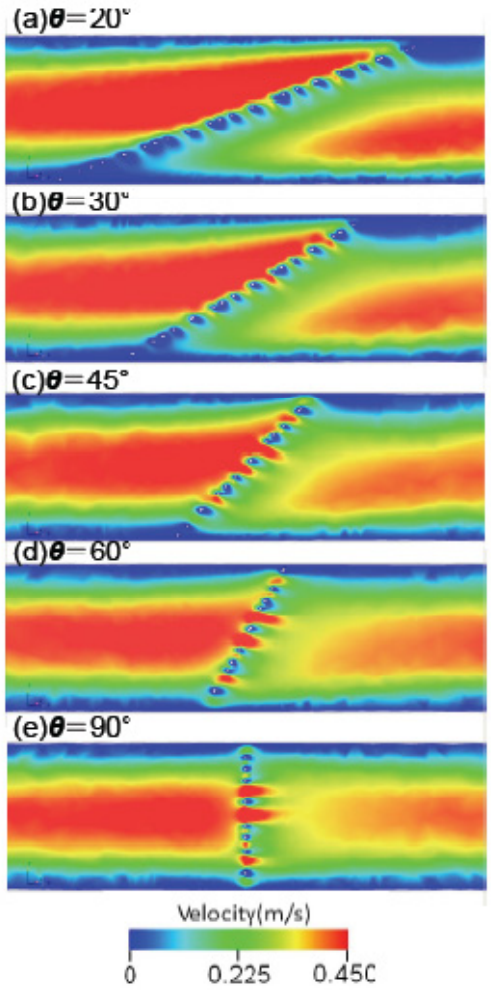

Fig. 12 Contour maps of velocity distribution in the center plane for inclined angles and parallel test section

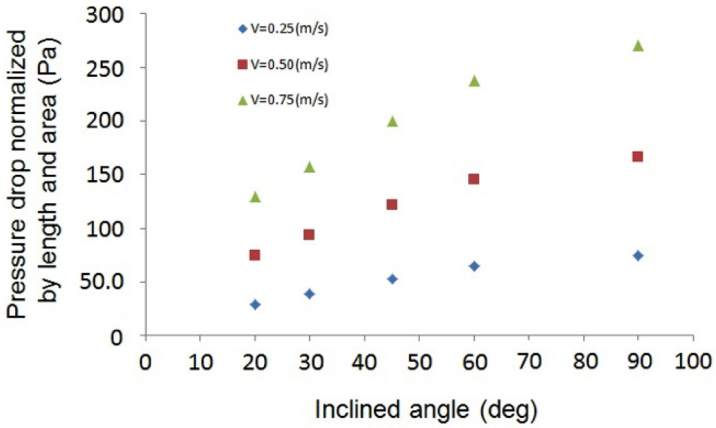

Fig. 13 Pressure drop per distance of calculation surfaces in test section with the area of struts

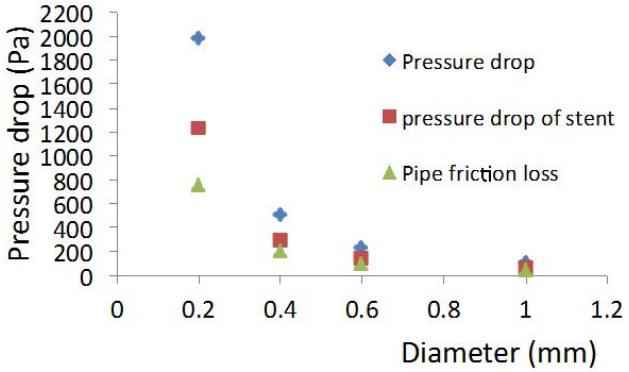

Fig. 14 Pressure drop in cylindrical test sections as a function of test section diameter

3.4 Pressure drop for inclined angles

Fig. 11 shows the pressure drop as a function of the inclined angle, and Fig. 12 shows contour maps of the velocity distribution in the center of the test section for several inclined angles. The results indicate that the pressure drop and higher velocity area increase as the stent inclines (i.e., for a larger inclined angle). This result should be related to the number of struts in the test section. With increasing inclined angle, the number of struts in the test section increases, which suggests that pressure drop depends on the angle at which the stent is inclined. We observe that the calculated pressure drop per strut decreases as the stent inclines (Fig. 13).

3.5 Cylindrical test section for parallel section

Fig. 14 shows the pressure drop in the cylindrical test section for the parallel direction as a function of cylinder diameter. The pressure drop decreases dramatically with increasing cylinder diameter. This result shows that the pressure drop depends on the diameter of the cylindrical test section. We further observe that pipe friction loss is moderately significant for test section diameters of 0.2 or 0.4 mm but becomes insignificant for diameters of 1 mm.

Fig. 15-1

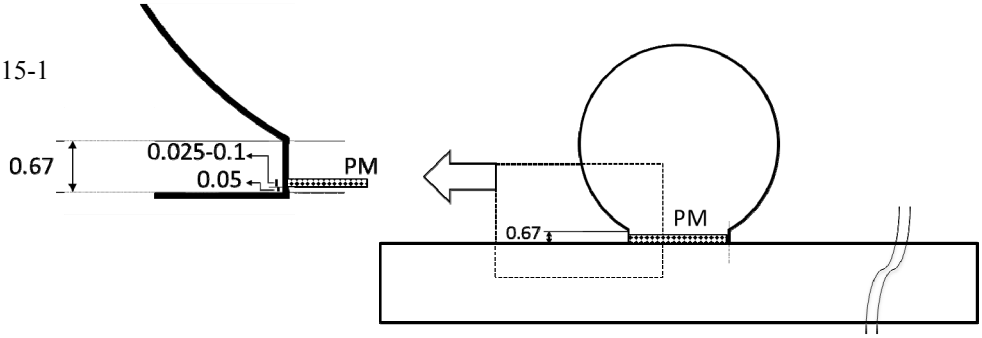

Fig. 15-2

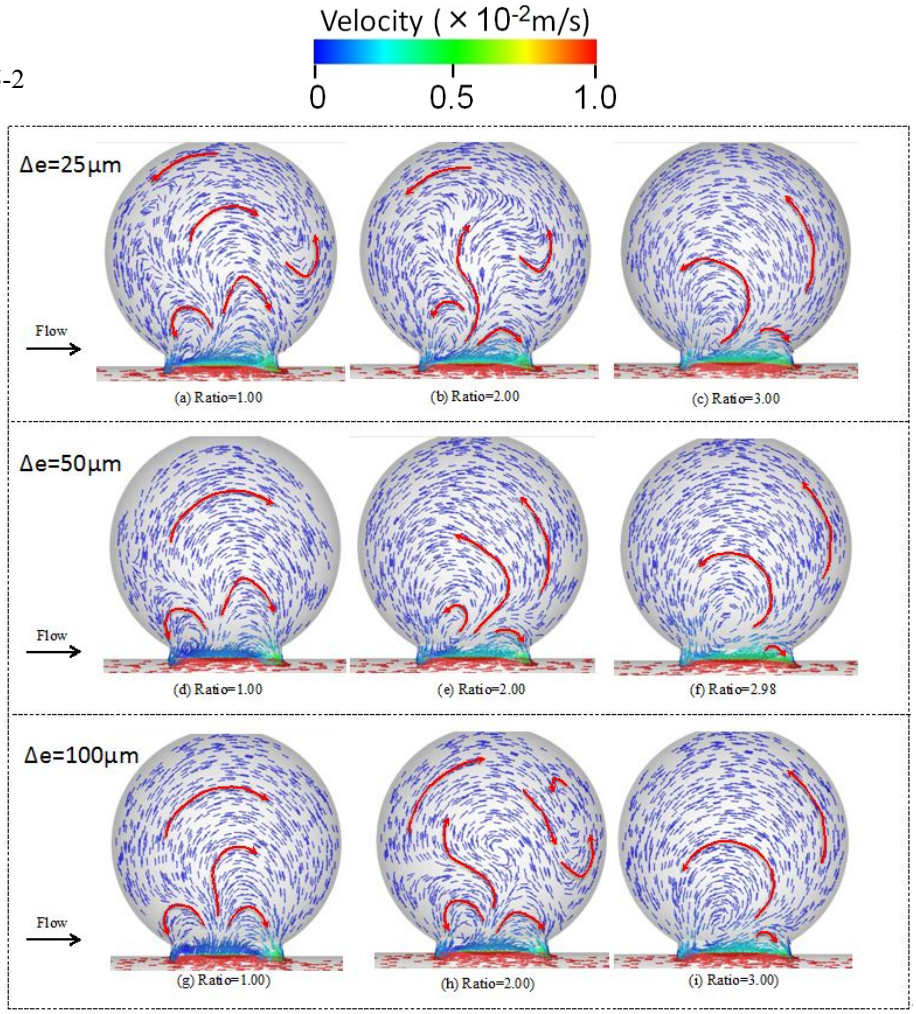

Fig. 15 Flow observation with PM with several ratio. Fig. 15-1 Position of PM in the neck (left is zoom-in from the right). Fig. 15-2 Flow patterns obtained using a PM with several permeability ratios

3.6 Ratio of parallel permeability to perpendicular permeability

Fig. 15 shows flow patterns for various ratios of parallel permeability to perpendicular permeability and for various PM thicknesses. Subjectively, the flow patterns are changed from a shower type (Fig. 15(a), (b)) to a bigger vortex rotating anticlockwise in accordance with increasing the ratio. And the flow pattern at the certain ratio is not the same if the thickness is changed.

For a smaller permeability ratio, perpendicular fluid flow is facilitated; therefore, fluid can enter the aneurysm more easily and the flow pattern is like a shower. For larger permeability ratios, fluid flow parallel to the aneurysm neck is facilitated and vortices are created in the aneurysm. On increasing the PM thickness, the perpendicular permeability decreases; therefore, the permeability ratio increases. These results indicate that the flow pattern when using a PM is affected by PM thickness and permeability ratio (parallel permeability to perpendicular permeability).

4. Discussion

This paper discusses stent models that use PMs and methods for calculating flow resistance. The results show that the calculation methods significantly affect the results, particularly in the parallel direction. Unlike the perpendicular direction, the method of computing parallel pressure drop (for defining a PM) is not yet fixed because the geometry of the test section strongly affects the results for pressure drop.

Several studies on pressure drop have been conducted in other fields, such as for bone marrow (Coughlin *et al*. 2012). In this study, bone marrow samples were cut into a cube or cylinder and the pressure drop was measured for a PM. In this case, the sample should have non-negligible thickness in every direction.

A stent, however, is thin (25-75 μm) and most stents have a layer of struts. In this case, parallel flow (through the stent) is difficult, as is measuring the parallel pressure drop. With the current method of using a rectangular test section (Augsburger *et al*. 2011), the parallel pressure drop depends on the size of the gap between the wall of the test section and the stent, and on the length of the stent. The results obtained in the present study with the cylindrical test section of various diameters reveal that pressure loss depends on tube friction. Therefore, the method introduced by Augsburger *et al*. (2011) to measure the parallel pressure drop can determine the pressure drop as one's mind by changing the length of the test section and the size of the gap between the wall of the test section and the stent.

A possible uniform method to measure parallel pressure drop was to incline the stent and extrapolate the pressure to 0°. However, the pressure drops obtained herein were too high; therefore, the normalized pressure drop per unit length is extremely small. In conclusion, the other way is necessary.

Furthermore, we examined how the ratio of parallel pressure drop to perpendicular pressure drop affects the flow pattern. The results reveal that the flow pattern is changed according to the ratio and the thickness. The smaller ratio shows a shower type, because the higher permeability of perpendicular thann the parallel makes a flow like shower at the aneurysmal neck. Then, a bigger vortex rotating anticlockwise is appeared in accordance with increasing the ratio because the parallel is higher than the perpendicular. Because PM thickness also affects the permeability based on Eq. (1), the thickness should affect not only the viscous resistance term (the reciprocal of permeability) but also the inertial resistance term.

However, if the PM has the same thickness as the stent, the parallel permeability may be determined as follows: First, determine the perpendicular pressure drop, then check the flow patterns for various permeability ratios and select a ratio for which the patterns are similar. Finally, use Eq. (3) to calculate the parallel permeability of the stent.

If the PM thickness differs from that of the stent, the calculation method should also be considered. If the stent is very thin, such as 25 μm, creating a mesh in a 25-μm-thick PM will be difficult. Thus, new techniques must be developed to create a mesh in thin PMs.

For practical use of PMs as stents, the inverse problem must be analyzed to observe the proper parallel pressure drop. Such an analysis can be expanded to categorize stents by permeability so that doctors can predict the flow reduction without resorting to computational simulation.

4.1 Limitations

This study involves several limitations and controversial issues. First, we used only a straight parent artery with a spherical aneurysm as an ideal model. The flow in the straight parent artery takes the form of a Poiseuille flow, and the flow patterns in the inflow zone (or bundle of inflow (Anzai *et al*. 2010)) are formed at the distal neck. The structure and flow patterns differ from a realistic flow pattern because the specific geometry of the patient will differ. Thus, the method proposed herein will be controversial for estimating flows in a real geometry. However, the geometry employed herein has been used for many years and the flow pattern of this geometry is well known, which facilitates the interpretation of first estimations based on this geometry.

The check of permeability of parallel and thickness using a curvature model will be also important for evaluation of PM. As Imai showed flow pattern of curvature models the angle of entering flow against the neck will depend on the curvature (Imai *et al*. 2008). Then, the flow patterns using curvature models with PM should be compared to a model with a real stent to find out the relation with the parameters of PM.

Future studies should consider the characteristics of blood flow such as non-Newtonian flow and pulsatile flow.

5. Conclusions

We present parametric studies of porous media applied as stents and investigate the resulting flow pattern with the aim of reducing the heavy computational load currently required for this task by fluid dynamics calculations. The results show that the test section used to compute the parallel pressure drop influences the permeability and flow patterns in the aneurysm. The computational method used to calculate the parallel flow can affect the resulting pressure drop across the stent. Using the permeability ratio and the perpendicular permeability, the parallel permeability may be obtained.

Acknowledgments

This study was partially supported by the Ministry of Education, Science, Sports and Culture, Grant-in-Aid for Scientific Research (B), 2013-2015(25282140, Makoto Ohta). This work was partly supported by the JSPS Core-to-Core Program, A.Advanced Research

Networks,"International research core on smart layered materials and structures for energy saving".

References

Anzai, H., Falcone, J.L., Chopard, B., Hayase, T. and Ohta, M. (2014), "Optimization of strut placement in flow diverter stents for four different aneurysm configurations", *J. Biomech. Eng.*, **136**(6), 0610061-0610067.

Anzai, H., Nakayama, T., Takeshima, Y. and Ohta, M. (2010), "The effect of 3D visualization on optimal design for strut position of intracranial stent", *Proceedings of the ASME*, **1**(FEDSM-ICNMM2010-30591), 1859-1867.

Anzai, H., Nakayama, T., Takeshima, Y. and Ohta, M. (2010), "The effect of 3D visualization on optimal design for strut position of intracranial stent", *Proceedings of the ASME 2010 3rd Joint US-European Fluids Engineering Summer Meeting and 8th International Conference on Nanochannels*, Microchannels, and Minichannels FEDSM-ICNMM2010 FEDSM-ICNMM2010-30591.

Augsburger, L., Reymond, P., Rufenacht, D.A. and Stergiopulos, N. (2011), "Intracranial stents being modeled as a porous medium: flow simulation in stented cerebral aneurysms", *Ann. Biomed. Eng*., **39**(2), 850-863.

Cebral, J.R., Mut, F., Raschi, M., Scrivano, E., Ceratto, R., Lylyk, P. and Putman, C.M. (2011), "Aneurysm rupture following treatment with flow-diverting stents: computational hemodynamics analysis of treatment", *Am. J. Neuroradiol*., AJNR, **32**(1), 27-33.

Coughlin, T.R. and Niebur, G.L. (2012), "Fluid shear stress in trabecular bone marrow due to low-magnitude high-frequency vibration", *J. Biomech*., **45**(13), 2222-2229.

Hassan, T., Timofeev, E.V., Saito, T., Shimizu, H., Ezura, M., Tominaga, T., Takahashi, A. and Takayama, K. (2004), "Computational replicas: anatomic reconstructions of cerebral vessels as volume numerical grids at three-dimensional angiography", *Am. J. Neuroradiol*., AJNR, **25**(8), 1356-1365.

Imai, Y., Sato, K., Ishikawa, T. and Yamaguchi, T. (2008), "Inflow into saccular cerebral aneurysms at arterial bends", *Ann. Biomed. Eng*., **36**(9), 1489-1495.

Karmonik, C., Chintalapani, G., Redel, T., Zhang, Y.J., Diaz, O., Klucznik, R. and Grossman, R.G. (2013), "Hemodynamics at the ostium of cerebral aneurysms with relation to post-treatment changes by a virtual flow diverter: A computational fluid dynamics study", *Conference of the Proceedings IEEE Eng. Med. Biol. Soc*., 1895-1898.

Kulcsar, Z., Augsburger, L., Reymond, P., Pereira, V. M., Hirsch, S., Mallik, A.S., Millar, J., Wetzel, S.G., Wanke, I. and Rufenacht, D.A. (2012), "Flow diversion treatment: intra-aneurismal blood flow velocity and WSS reduction are parameters to predict aneurysm thrombosis", *Acta Neurochir (Wien)*, **154**(10), 1827-1834.

Lee, C.J., Srinivas, K. and Qian, Y. (2014), "Three-dimensional hemodynamic design optimization of stents for cerebral aneurysms", *Proceedings of the Institution of Mechanical Engineering Part. H*, **228**(3), 213-224.

Ma, D., Dargush, G.F., Natarajan, S.K., Levy, E.I., Siddiqui, A.H. and Meng, H. (2012), "Computer modeling of deployment and mechanical expansion of neurovascular flow diverter in patient-specific intracranial aneurysms", *J. Biomech*., **45**(13), 2256-2263.

Sadasivan, C., Cesar, L., Seong, J., Wakhloo, A.K. and Lieber, B.B. (2009), "Treatment of rabbit elastase-induced aneurysm models by flow diverters: development of quantifiable indexes of device performance using digital subtraction angiography", *IEEE Trans. Med. Imaging*, **28**(7), 1117-1125.

Xu, J., Deng, B., Fang, Y., Yu, Y., Cheng, J., Wang, S., Wang, K., Liu, J.M. and Huang, Q. (2013), "Hemodynamic changes caused by flow diverters in rabbit aneurysm models: Comparison of virtual and realistic FD deployments based on Micro-CT reconstruction", *PLoS One*, **8**(6), e66072.

Yujie Li, Anzai, Hitomi, Nakayama, Toshio, Shimizu, Yasumoto, Miura, Yukihisa, Qiao, Aike and OHTA, M. (2014), "Simulation of hemodynamics in artery with aneurysm and stenosis with different geometric configuration", *J. Biomech. Sci. Eng*., **9**(1), JBSE0003.

Zhang, Y., Chong, W. and Qian, Y. (2013), "Investigation of intracranial aneurysm hemodynamics following flow diverter stent treatment", *Med. Eng. Phys*., **35**(5), 608-615.

YC